The redox state of the plastoquinone (PQ) pool is connected to thylakoid lipid saturation in a marine diatom

Kuan Yu Cheong, Juliette Jouhet, Eric Maréchal, Paul G Falkowski

Title: The redox state of the plastoquinone (PQ) pool is connected to thylakoid lipid saturation in a marine diatom

Kuan Yu Cheong[1,2] (ORCID: 0000-0002-9118-5797), Juliette Jouhet[3], Eric Maréchal[3] and Paul G. Falkowski[1,2,4]

[1]Environmental Biophysics and Molecular Ecology Program, Department of Marine and Coastal Sciences, Rutgers, The State University of New Jersey, New Brunswick, NJ 08901

[2]Department of Plant Biology, Rutgers, The State University of New Jersey, New Brunswick, NJ 08901

[3]Laboratoire de Physiologie Cellulaire et Végétale, Unité Mixte Recherche 5168, Centre National Recherche Scientifique, Commissariat à l'Energie Atomique et aux Energies Alternatives, INRAE, Université Grenoble Alpes, Grenoble Cedex 9, France

[4]Department of Earth and Planetary Sciences, Rutgers, The State University of New Jersey, Piscataway, NJ 08854

Author of correspondence

Paul G. Falkowski; falko@marine.rutgers.edu

Abstract

The redox state of the plastoquinone (PQ) pool is a known sensor for retrograde signaling. In this paper, we asked, "does the redox state of the PQ pool modulate the saturation state of thylakoid lipids?" Data from fatty acid composition and mRNA transcript abundance analyses suggest a strong connection between these two phenomena in a model marine diatom. Fatty acid profiles of *Phaeodactylum tricornutum* exhibited specific changes when the redox state of the PQ pool was modulated by light and two chemical inhibitors 3-(3,4-dichlorophenyl)-1,1-dimethylurea (DCMU), which leads to the oxidation of the PQ pool, or 2,5-dibromo-3-methyl-6-isopropyl-p-benzoquinone (DBMIB), which leads to the reduction of PQ. Data from liquid chromatography with tandem mass spectrometry (LC-MS/MS) indicated a *ca.*7-20% decrease in the saturation state of all four conserved thylakoid lipids in response to an oxidized PQ pool. The redox signals generated from an oxidized PQ pool in plastids also increased the mRNA transcript abundance of nuclear-encoded C16 fatty acid desaturases (FADs), with peak upregulation on a timescale of 6 to 12 h. These results strongly suggest the presence of a retrograde signaling pathway. The connection between the redox state of the PQ pool and thylakoid

lipid saturation suggests a heretofore unrecognized signaling pathway that couples photosynthetic electron transport and the physical state of thylakoid membrane lipids.

Key words (alphabetical): Diatom, Lipid saturation, PQ pool, Redox state, Retrograde signaling, Thylakoid membrane

Introduction

Light and temperature affect the flux of excitation energy and photosynthesis, but how a plant cell responds to these environmental signals is not well understood. In eukaryotic algae, more than 90% of the proteins in the plastid are encoded in the nucleus (Abdallah et al., 2000; Allen et al., 2011; Grzebyk et al., 2003; Martin et al., 2002; Rujan & Martin, 2001). As the plastidome possesses only minimal set of genes to support photosynthesis (Oudot-Le Secq et al., 2007; Valentin et al., 1992), eukaryotic photosynthetic cells evolved retrograde signaling mechanisms that facilitate environmental cues between nuclear gene expression and proteins in the plastid. In this paper, we examine a potential signaling pathway responsible for thylakoid lipid saturation in a model marine diatom.

The oxidation of plastoquinol (PQH_2) at the Q_0 site of cytochrome b_6f complex (cyt b_6f) is the slowest step in linear photosynthetic electron transport (PET) (Haehnel, 1977). Hence, the redox state of the plastoquinone (PQ) pool can potentially generate a redox signal to reflect the fluctuation in PET induced by environmental factors. In response to changes in light intensity, the redox state of the PQ pool regulates the expression of nuclear-encoded genes responsible for light harvesting pigment protein complexes (Chen et al., 2004; Escoubas et al., 1995; Yang et al., 2001). Similarly, the expression of nuclear-encoded pigment protein complexes is affected by changes in temperature, which also has been associated with the redox state of the PQ pool (Denis P. Maxwell et al., 1994). Furthermore, the redox state of the PQ pool transcriptionally regulates the stoichiometry of photosystem II (PSII) and photosystem I (PSI) in cyanobacteria, green algae and terrestrial plants (Karpinski et al., 1997; Li & Sherman, 2000; D. P. Maxwell et al., 1995; Pfannschmidt et al., 1999). Are there other cellular processes regulated by the redox state of the PQ pool?

The lipid composition in the plastid is characterized by a high abundance of non-phosphate containing glycoglycerolipids including sulfoquinovosyldiacylglycerol (SQDG), monogalactosyldiacylglycerol (MGDG) and digalactosyldiacylglycerol (DGDG), as well as a low abundance of phosphoglycerolipids, such as phosphatidylglycerol (PG), phosphatidylcholine (PC) and phosphatidylinositol (PI) (Block et al., 1983; Douce et al., 1987; Mendiola-Morgenthaler et al., 1985).

Among them, SQDG, MGDG, DGDG and PG make up the four conserved lipids in thylakoid membranes in all oxygenic photoautotrophs. The acyl tails of these lipids are enriched in long-chain, unsaturated fatty acids and their saturation state heavily influences the viscosity of the hydrophobic membrane core (Harwood & Jones, 1989; Sarcina et al., 2003). For instance, an increase in thylakoid fatty acid saturation inhibits the rate of linear photosynthetic electron transport (PET) (Horváth et al., 1986; Öquist, 1982; Vigh et al., 1985). Decreasing fatty acid saturation is also connected to an increase in diffusion of quinone, a PQ-like lipophilic mobile electron carrier in mitochondrial respiration (Budin et al., 2018). Furthermore, thylakoid membranes are devoid of sterols (Nakamura & Li-Beisson, 2016). Without sterols to promote membrane cohesion, these membranes are especially susceptible to environmental conditions that alter their physical states (Beck et al., 2007; Dufourc, 2008a, 2008b). Therefore, a robust and rapid retrograde signaling mechanism is crucial to maintain an optimal biophysical state of thylakoid membranes for photosynthesis. However, little is known about the initial signals that trigger the modulation of the saturation state of thylakoid lipids. This knowledge gap is especially wide in diatoms, a group of unicellular eukaryotic photoautotrophs that often dominate in polar and temperate seas. In this paper, we tested the hypothesis that diatoms could alter the saturation state of their thylakoid lipids through a signal generated from the redox state of the PQ pool.

We present evidence that the redox state of the PQ pool is connected to thylakoid fatty acid saturation. Data from GC-MS analyses revealed that the fatty acid profiles, especially C16 fatty acids, exhibited specific changes in abundance when the PQ pool redox state was modulated independently by light or chemical inhibitors. Further examination with an oxidized PQ pool revealed: 1) decreases in the saturation state of all conserved thylakoid lipids and 2) increases in the mRNA transcript abundance of nuclear-encoded C16 fatty acid desaturase (FADs). These findings strongly suggest the presence of a retrograde signaling pathway that regulates the fluidity of thylakoid membranes.

Materials and methods

Culture maintenance, cell count and treatment

Phaeodactylum tricornutum Bohlin (CCAP 1055/1; strain Pt1 8.6) was maintained axenically in batch in artificial seawater enriched to F/2 levels at 18°C (R. R. Guillard, 1975; R. R. Guillard & Ryther, 1962). Cells were grown under a 14/10 h light/dark cycle with white light emitting diodes at 500 µmol photons m^{-2} s^{-1} and 20 µmol photons m^{-2} s^{-1} for high-light and for low-light acclimated cells, respectively. Cells used in all experiments were diluted to maintain log growth phase for at least three

consecutive generations (R. R. L. Guillard, 1973; Sunda et al., 2005). Cell densities were quantified using a Beckman Coulter Multisizer 3 (Beckman Coulter).

To oxidize the PQ pool of the cells, high-light acclimated cells were either shifted to the low light condition or incubated with sublethal concentrations of 3-(3,4-dichlorophenyl)-1,1-dimethylurea (DCMU; dissolved in absolute ethanol; Tokyo Chemical Industry) for 24 h. Conversely, low-light acclimated cells were shifted to the high light condition or incubated with sublethal concentrations of 2,5-dibromo-3-methyl-6-isopropyl-p-benzoquinone [DBMIB; dissolved in dimethyl sulfoxide (DMSO); Sigma-Aldrich] for equal amount of time to reduce the PQ pool (Durnford et al., 1998). We defined "sublethal concentrations" as the doses of DCMU and DBMIB that decreased growth rate, but still allowed photochemical activity (Figure 3). Doses which resulted in negative growth rate were excluded from analysis to prevent interference from the toxic effects. If not otherwise indicated, 25 nM of DCMU and 1.2 DBMIB were used in this study. All experiments were conducted at around 6 h after first light to minimize inteference from circadian rhythm and photoperiod.

Fatty acid composition analysis

For total cellular fatty acid analysis [i.e., fatty acids methyl esters (FAMEs)], cells were harvested by filtration with glass fiber filters (GF/F; Whatman), followed by lipid extraction and transesterification (Bligh & Dyer, 1959; Rodríguez-Ruiz et al., 1998). The FAMEs were analyzed using a Shimadzu GC-MS-QP2010S Gas Chromatography Mass Spectrometer (GC-MS; Shimadzu Scientific Instruments) equipped with a TRACE™ TR- FAME GC Column (60 m × 0.25 mm, film thickness 0.25 µm; Thermo Fisher Scientific), FID detector and quadrupole mass spectrometer. All detectable FAME species were identified by comparing the mass spectra to the National Institute of Standards and Technology 11 library. The relative abundance of each FAME species was corrected for extraction efficiency (Jenke & Odufu, 2012), quantified by referencing to a known amount of heptadecanoic acid internal standard (Sigma- Aldrich), and expressed as molecular percentage of total fatty acid. The double bond index (DBI) was determined with all detectable fatty acid species as described (Feijão et al., 2017).

We used liquid chromatography with tandem mass spectrometry (LC-MS/MS) to quantify fatty acids by lipid headgroups on the LIPANG platform, Grenoble, France, as described (Jouhet et al., 2017). Briefly, lipid extracts corresponding to 25 nmol of total fatty acids were dissolved in 100 µL of chloroform/methanol [2:1, (v/v); containing 125 pmol of each internal standard]. The internal standards were phosphatidylethanolamine (PE) 18:0-18:0 (Avanti Polar Lipid), diacylglycerol (DAG) 18:0-22:6 (Avanti Polar Lipid) and SQDG 16:0-18:0 extracted from spinach thylakoids (Demé et al., 2014) and

hydrogenated (Buseman et al., 2006). The lipid extract was separated in lipid classby HPLC (Rainteau et al., 2012) and quantified by MS/MS. The HPLC separation was performed at 40°C using an Agilent 1200 HPLC system equipped with a 150 mm × 3 mm (length × internal diameter) 5 µm diol column (Macherey-Nagel). The distinct glycerophospholipid classes were eluted successively as a function of the polar head group. The mass spectrometric analysis was done on a 6460 triple quadrupole mass spectrometer (Agilent) equipped with a Jet stream electrospray ion source. This quantification was done by multiple reaction monitoring (MRM) with 50 ms dwell time. Lipid amounts (pmol) were corrected for response differences between internal standards and endogenous lipids and by comparison with a quality control (QC). The QC extract, corresponding to a known *Phaeodactylum* lipid extract, was qualified and quantified by TLC and GC-FID (Jouhet et al., 2017).

Fast repetition rate (FRR) fluorescence measurement of PSII

DCMU irreversibly binds to the Q_b site of PSII and blocks electron input into the PQ pool i.e., oxidizing the PQ pool (Fedtke, 1982; Trebst, 2007). The inhibitory effect of DCMU was assessed by the time constant of Q_a reoxidation (τ_{Qa}), determined by a three-component analysis on the fluorescence relaxation kinetics after a single turnover flash, using a custom built, miniaturized Fluorescence Induction and Relaxation (mini-FIRe) instrument (Gorbunov & Falkowski, 2020; Kolber et al., 1998).

mRNA transcript abundance analysis

For quantitative reverse transcription PCR (RT-qPCR) analysis, total cellular RNA was extracted using TRIzol Reagent (Invitrogen). The extracted RNA was purified by using a RNeasy MinElute Cleanup Kit (Qiagen). RT-qPCR was performed using an Applied Biosystem High-Capacity cDNA Reverse Transcription Kit (Thermo Fisher Scientific) and Power SYBR Green Master Mix (Thermo Fisher Scientific). Primers for the qPCR reaction were designed using Primer Express Software v3.0.0 (Thermo Fisher Scientific) and listed in Table S1. The reactions were assessed using a QuantStudio 3 Real-Time PCR System. The ribosomal protein small subunit 30S (RPS) gene was used as an internal standard (Siaut et al., 2007). The relative mRNA expression ratio (R) of C16 fatty acid desaturases (FADs) was expressed according to (Pfaffl, 2001).

Pigment composition analysis

Cells were harvested by filtration with GF/F filters (Whatman). The samples were wrapped in foil and flash frozen at −80 °C in liquid nitrogen. Pigment extraction and high-performance liquid chromatography (HPLC) analysis were performed as described (Wright et al., 1991). Briefly, pigment composition was analyzed with an Agilent 1100/1200 series HPLC system equipped with a G1315C Diode

Array Detector (scanning wavelengths 275-800 nm) and Zorbax Eclipse Plus C18 column (4.6x250mm; 5 µm). The following HPLC Grade phase eluents were used: Solvent A (80% Methanol, 20% aqueous Ammonium Acetate, pH 7.2); Solvent B (90% Acetonitrile, 10% Water); Solvent C (100% Ethyl Acetate). Peaks were quantified at 440 nm. Pigments were identified automatically using the Agilent software, based on retention time and spectral shape. All peak area quantification and pigment idenfication were manually verified.

Statistical analysis

Normality was assumed in all analyses. Homoscedasticity of data was evaluated with the Levene test. If homoscedastic, an independent Student's t-test was performed (Section 3.1, 3.3-3.6; scipy.stats.ttest_ind, v1.6.2); otherwise, the Mann-Whitney U test was used (Section 3.3 and 3.5; scipy.stats.mannwhitneyu, v.1.6.2). One- way analysis of variance (ANOVA) was performed, followed by pairwise Tukey- HSD post-hoc test in Section 3.2 using a Python statistical package, Pingouin version 0.33 (Vallat, 2018). All tests were performed at $\alpha = 0.05$.

Results

Total cellular fatty acid profiles

Fatty acid profiles exhibited specific changes depending on the redox state of the PQ pool (Fig. 1). 12 out of the 14 fatty acid species (ca. 85%) responded identically, suggesting that an oxidized PQ pool modulates fatty acid abundance. When the PQ pool is reduced by high light or DBMIB, 11 out of 14 (ca. 80%) fatty acid species responded in an identical manner. Data suggest that fatty acids respond in opposite directions depending on the redox state of the PQ pool (Fig. 2). Specifically, the FAs responsible for the changes were C16:0, C16:1, C16:2, C16:3, C16:4, C20:5, C24:0 and C22:6. Among these "redox sensitive" FAs, C16:0, C16:1, C16:2 and C16:4 exhibited significant and specific changes in response to the redox state of the PQ pool.

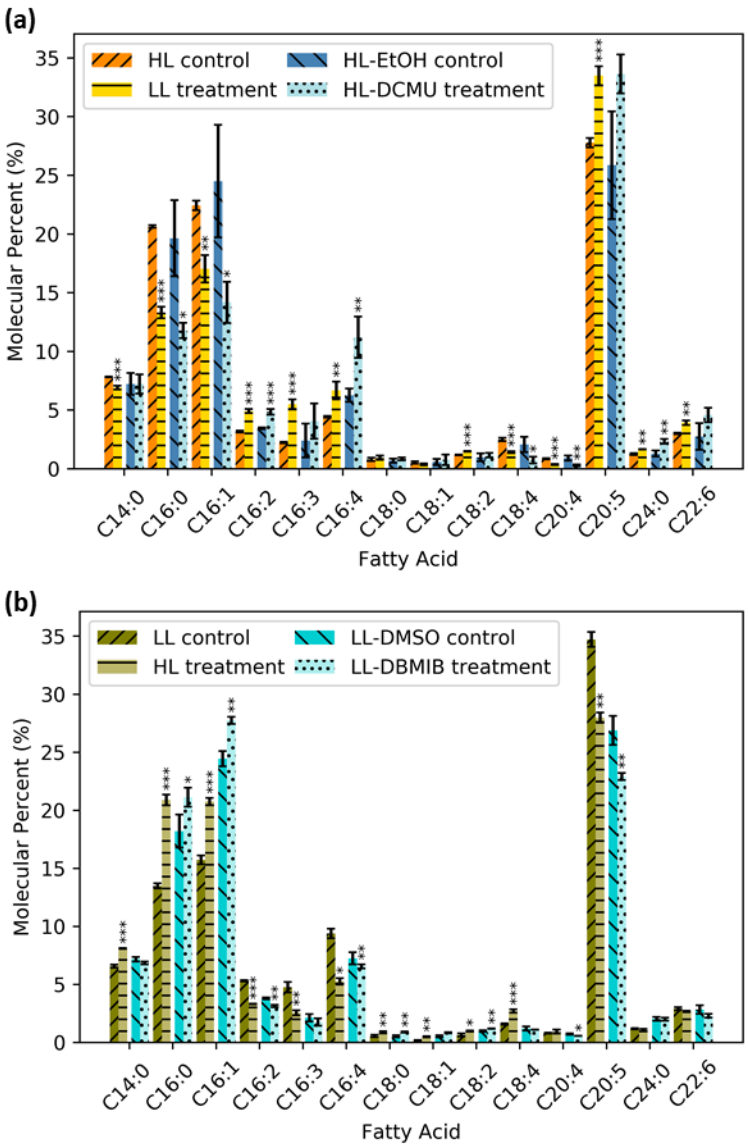

175

176 **Fig. 1. Cellular fatty acid profiles of *P. tricornutum* measured by gas chromatography-mass**
177 **spectrometry (GC-MS).** (a) Oxidation of the PQ pool with low light (LL) and 3-(3,4-dichlorophenyl)-1,1-
178 dimethylurea (DCMU) treatments for 24 h (b) Reduction of the PQ pool with high light (HL) and 2,5-
179 dibromo-3-methyl-6-isopropyl-p-benzoquinone (DBMIB) treatments for 24 h. Values reported are
180 means ± standard deviation (n = 3 biological replicates; except for HL treatment where n = 2). "*"
181 represents $p \leqslant 0.05$, "**" represents $p \leqslant 0.01$ and "***" represents $p \leqslant 0.001$ ($\alpha = 0.05$ with
182 independent t-test).

Fatty acid species	Direction of change relative to control			
	Oxidized PQ pool		Reduced PQ pool	
	LL	*DCMU*	*HL*	*DBMIB*
C14:0	Down***	Unchanged	Up***	Down
C16:0	**Down*** **	**Down***	**Up*** **	**Up***
C16:1	**Down****	**Down***	**Up*** **	**Up****
C16:2	**Up*** **	**Up*** **	**Down*** **	**Down****
C16:3	Up***	Up	Down**	Down
C16:4	**Up****	**Up****	**Down***	**Down****
C18:0	Up	Up	Up**	Up**
C18:1	Down	Up	Up**	Up
C18:2	Up***	Up	Up*	Up**
C18:4	Down***	Down*	Up***	Unchanged
C20:4	Down***	Down**	Unchanged	Down*
C20:5	Up***	Up	Down**	Down**
C24:0	Up**	Up**	Down	Down
C22:6	Up**	Up	Down	Down

Fig. 2. Changes in fatty acid abundance in response to the redox state of the PQ pool. The direction of change reported after 24 h of treatments are derived from values reported in Fig. 1. Fatty acid species with significant opposite directions of change in oxidized versus reduced PQ pool are in bold. "*" represents $p \leqslant 0.05$, "**" represents $p \leqslant 0.01$ and "***" represents $p \leqslant 0.001$ at $\alpha = 0.05$ with independent t-test (n = 3 biological replicates; except for HL treatment where n = 2 biological replicates).

The saturation state of cellular fatty acids

We hypothesized that an oxidized PQ pool would lead to a decrease in the fatty acid saturation. Indeed, increased concentrations of DCMU led to increased DBIs (Fig. 3a). Relative to the control, DBI increased by 20.5%, 22.4%, 22.4% and 29.2%, as τ_{Qa} increased by 125.1%, 159.0%, 194.0% and 312.0%. Among the "redox sensitive" fatty acids, the abundance of C16:0 and C16:1 significantly decreased as the concentration of DCMU increased (Fig. 3b). On the other hand, the abundance of less saturated C16:2 and C16:4, and longer C24:0 significantly increased.

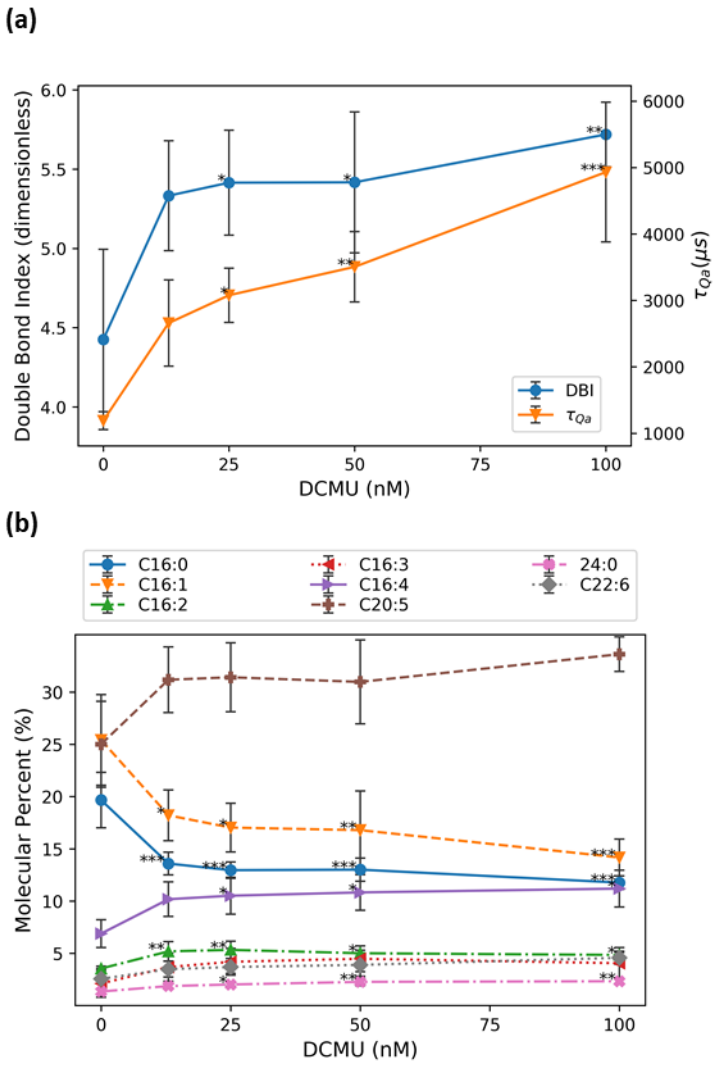

198

199 **Fig. 3. Fatty acid saturation state and abundance as a function of DCMU concentration.** (a) The double
200 bond index (DBI) and time constant of Qa reoxidation (τ_{Qa}), as a function of 3-(3,4-dichlorophenyl)-1,1-
201 dimethylurea (DCMU) concentration. DBI was computed from all detectable fatty acid species. (b) Fatty
202 acid abundance as a function of DCMU. The "redox sensitive" fatty acids identified in Fig. 2 are included
203 for brevity. Values reported are means ± standard deviation (n = 3 biological replicates). "*" represents p
204 $\leqslant$ 0.05, "**" represents p $\leqslant$ 0.01 and "***" represents p $\leqslant$ 0.001 (α = 0.05 with one-way ANOVA and
205 Tukey-HSD post-hoc test).

206

The saturation state of thylakoid lipids

The saturation state of thylakoid glycerolipids i.e., SQDG, MGDG, DGDG and PG, increased when the PQ pool was kept oxidized by DCMU (Fig. 4a). The DBI of non-thylakoid lipids such as PC, DAG and TAG were also affected, with their DBIs significantly increased by 6.7%, 6.1% and 27.0%, respectively. However, this increase in DBI seems to be specific. The DBI of PI, PE and DGTA were unchanged by an oxidized PQ pool. C16 fatty acids and C20:5 appear to contribute to most of the observed changes. C16:2 (45.9%) appeared to be the main contributor of the increase in SQDG (Fig. 4b). The largest significant changes observed in MGDG were C16:1 (-72.1%), C16:4 (34.3%) and C20:5 (22.2%; Fig. 4c). For DGDG, they were C16:1 (-35.3%), C16:2 (28.1%) and C20:5 (39.8%; Fig. 4d). Increase in DBI of PG could be mostly attributed to C16:0 (-26.7%) and C20:5 (32.9%; Fig. 4e). In TAG, C16:0 (-17.2%) and C20:5 (101.9%) led to the increase in the DBI.

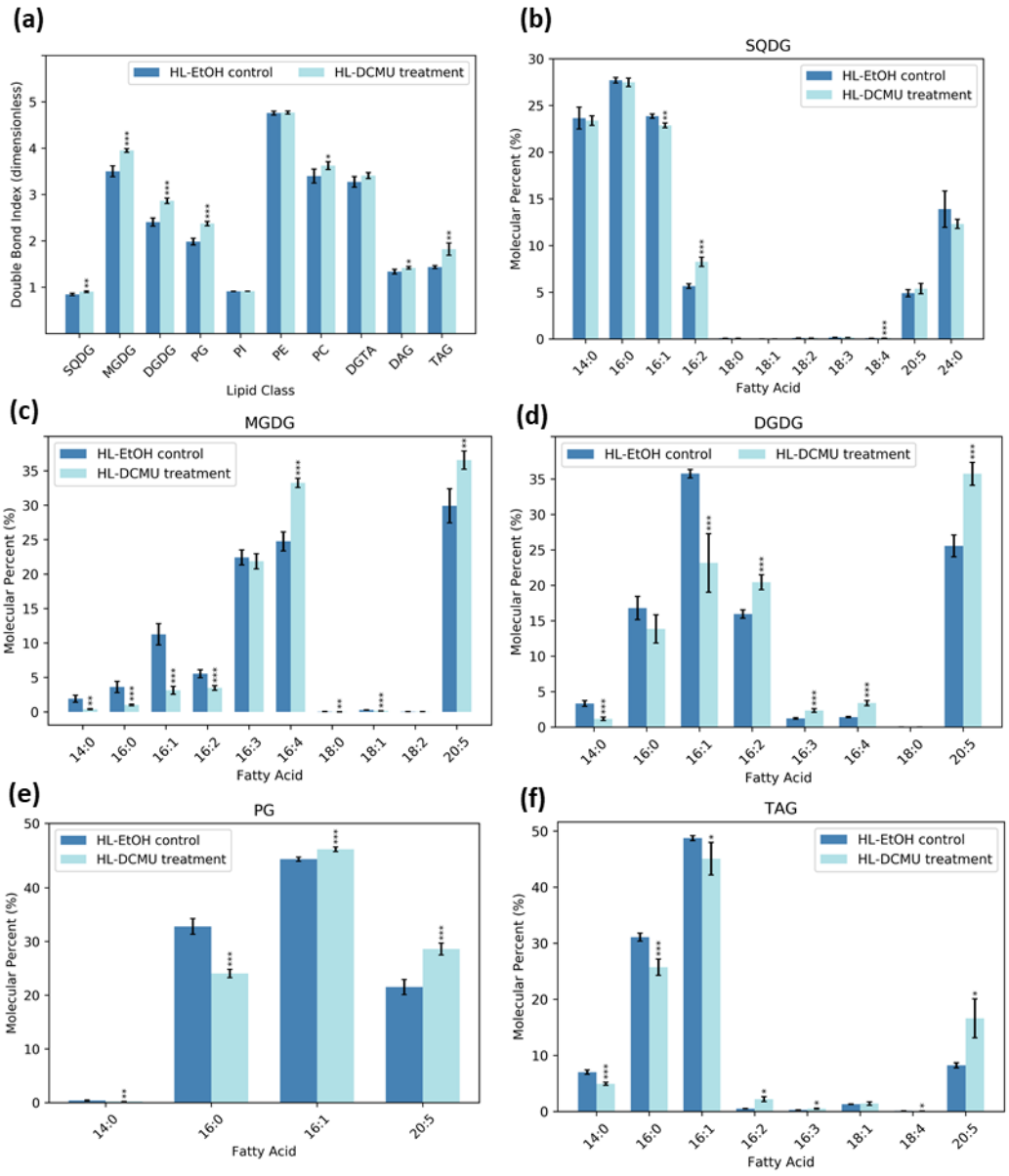

Fig. 4. The double bond index (DBI) of *P. tricornutum* measured by liquid chromatography with tandem mass spectrometry (LC-MS/MS) (a) DBI of all detectable lipid species in diatoms treated with ethanol (EtOH; carrier control) and 25 nM of 3-(3,4-dichlorophenyl)-1,1-dimethylurea (DCMU) for 24 h are reported (b) DBI of (b) SQDG (c) MGDG (d) DGDG (e) PG (f) TAG fatty acid tails. Values reported are means ± standard deviation (n = 4 biological replicates). "*" represents $p \leqslant 0.05$, "**" represents $p \leqslant 0.01$ and "***" represents $p \leqslant 0.001$ ($\alpha = 0.05$ with independent t-test for homoscedastic data and Mann–Whitney U test for non-homoscedastic data). Abbreviations: SQDG, sulfoquinovosyldiacylglycerol; MGDG, monogalactosyldiacylglycerol; DGDG, digalactosyldiacylglycerol; PG, phosphatidylglycerol; PI, phosphatidylinositol; PE, phosphatidylethanolamine; PC,

phosphatidylcholine; DGTA, diacylglyceryl hydroxymethyltrimethyl-β-alanine; DAG, diacylglycerol; TAG, triacylglycerol.

mRNA transcripts of C16 fatty acid desaturases

To examine if there is a connection between an oxidized PQ pool and nuclear-encoded FADs related to C16 fatty acids, we examined the transcription of the potential proteins. In *P. tricornutum*, the FAD PAD (palmitoyl-ACP desaturase; Phatr3_J9316) is located on chromosome 1; PTD12 (Phatr3_J48423) on chromosome 17; Putative C16:2 to C16:3 desaturase (Phatr3_EG02619) on chromosome 30; and PTD15 (Phatr3_J41570) on chromosome 31. Is the redox state of the PQ pool connected to the transcription of these genes?

RT-qPCR measurements revealed that within 6 h of PQ pool oxidation there was a threefold increase in the transcription of the PAD, involved in the C16:0 to C16:1 desaturation, and a 1.6-fold increase in the putative C16:2 to C16:3 desaturase. At 12 h, most FADs were significantly upregulated, i.e., PAD by 2.6-fold; PTD12 by 3.4-fold and putative C16:2 to C16:3 desaturase by 2.3-fold. PTD15 was upregulated by almost 10-fold, despite the large standard deviation. It appears that this putative retrograde signaling pathway functions on a time scale of 6 to 12 h. 24 h of incubation did not significantly change the Rs of FADs tested.

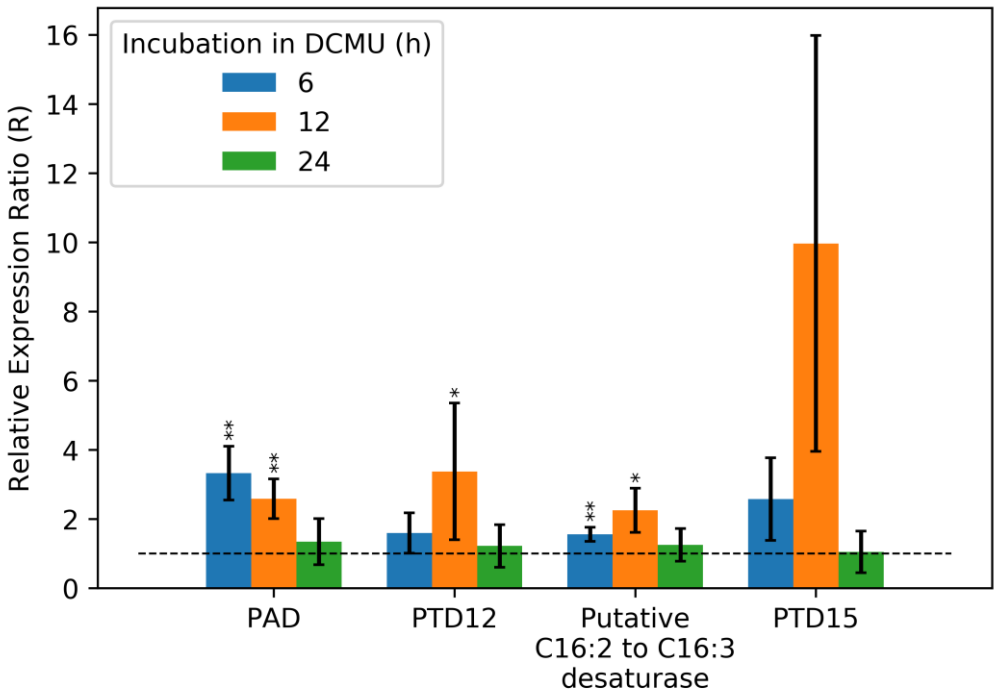

Fig. 5. Relative mRNA expression ratio (R) of C16 fatty acid desaturases (FADs) after incubation in 25 nM of DCMU for 6, 12 and 24 h. R of a FAD is expressed in comparison to an internal standard ribosomal protein small subunit 30S (RPS) gene (Siaut et al., 2007), in DCMU treatments versus respective carrier controls (ethanol) according to (Pfaffl, 2001). We referred to Dolch & Maréchal (2015) and Smith et al., (2021) for the function of each FAD. Dashed line at R of 1 indicates no change in expression level. Values reported are means ± standard deviation (n = 3 biological replicates, except for PTD15 where n = 4 biological replicates). "*" represents $p \leqslant 0.05$ and "**" represents $p \leqslant 0.01$ ($\alpha = 0.05$ with independent t-test between target gene and RPS). Gene name (function) and Ensembl Protists ID: PAD (desaturates C16:0 to C16:1), Phatr3_J9316; PTD12 (desaturates C16:1 to C16:2), Phatr3_J48423; Putative C16:2 to C16:3 desaturase, Phatr3_EG02619; PTD15 (desaturates C16:3 to C16:4), Phatr3_J41570.

Diatom lipid composition

In addition to the saturation state of thylakoid fatty acids, lipid composition can affect thylakoid structure and function by lipid phase behaviors. Thus, we examined if an oxidized PQ pool can modulate thylakoid lipid composition. Among the quartet of conserved thylakoid lipids, we observed significant changes only in DGDG (-63.0% relative to control; Fig. 6a) that led to an increased in MGDG/DGDG (Fig. 6b). The charge distribution of thylakoid membranes i.e., neutral/anionic lipids, and composition of negatively charged lipids (SQDG and PG) appeared to be unchanged by the oxidation state of the PQ pool (Fig. 6b). Other lipids exhibiting significant changes include PC (43.4%), DGTA (15.5%), DAG (-49.8%) and TAG (-91.7%; Fig. 6a).

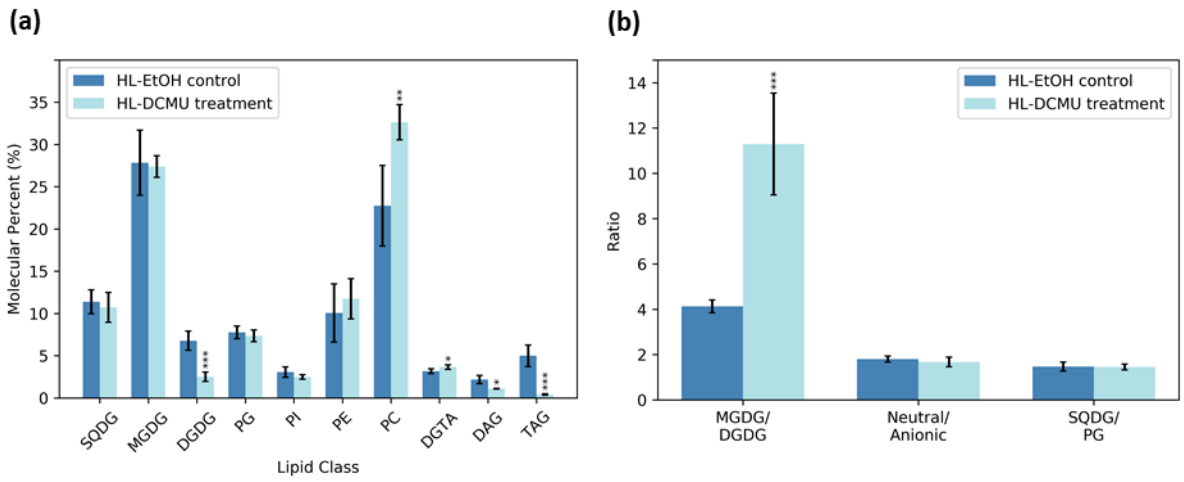

Fig. 6. Lipid composition of *P. tricornutum* measured by liquid chromatography with tandem mass spectrometry (LC-MS/MS) (a) Sum of molecular abundance by lipid category. Diatom cells were treated with ethanol (EtOH; carrier control) and 25 nM of 3-(3,4-dichlorophenyl)-1,1-dimethylurea (DCMU) for 24 h (b) The ratios of lipid classes. Neutral: MGDG and DGDG; Anionic: SQDG and PG. Values reported are means ± standard deviation (n = 4 biological replicates). "*" represents $p \leqslant 0.05$, "**" represents $p \leqslant 0.01$ and "***" represents $p \leqslant 0.001$ ($\alpha = 0.05$ with independent t-test with homoscedastic data; Mann–Whitney U test for non-homoscedastic data). Abbreviations: SQDG, sulfoquinovosyldiacylglycerol; MGDG, monogalactosyldiacylglycerol; DGDG, digalactosyldiacylglycerol; PG, phosphatidylglycerol; PI, phosphatidylinositol; PE, phosphatidylethanolamine; PC, phosphatidylcholine; DGTA, diacylglyceryl hydroxymethyltrimethyl-β-alanine; DAG, diacylglycerol; TAG, triacylglycerol.

Discussion

Although the environmental cues (e.g., light and temperature) that trigger modulation of fatty acid saturation are known, the initial sensing signal(s) remains elusive. It is well established that the redox state of the PQ pool can generate retrograde signals to regulate photosynthetic pigments and proteins on the order of minutes to days in cyanobacteria, green algae, diatoms and terrestrial green plants (Escoubas et al., 1995; Karpinski et al., 1997; Lepetit et al., 2012; Li & Sherman, 2000; D. P. Maxwell et al., 1995; Pfannschmidt et al., 1999). In this work, we examined the hypothesis that the redox state of the PQ pool modulates the saturation state of thylakoid fatty acids. Our results strongly suggest a connection between these two phenomena.

There was a *ca.* 85% agreement in changes of fatty acid abundance between LL and DCMU treatments i.e., an oxidized PQ pool. Reduction of the PQ pool by HL or DBMIB treatments resulted in a *ca.* 80% agreement in directions of abundance change (Fig. 1 and 2). DCMU treatments resulted in increased τ_{Qa} (Fig. 3a) and, by inference, a more oxidized PQ pool. Thus, it appears oxidation of the PQ pool is connected to the increase in DBI. To definitively examining the role of the redox state of the PQ pool in thylakoid lipid modulation, future studies might include direct HPLC measurement of PQ, as demonstrated in (Khorobrykh et al., 2020). Nevertheless, biophysical analysis of the redox state of the PQ pool has been used for more than 40 years(Diner & Joliot, 1976). Our data suggest a strong corrleation between total cellular DBI in thylakoid lipids and the redox state of the PQ pool.

Besides the four conserved thylakoid lipids, the DBI of DAG, TAG and PC also significantly increased. DAG serves as a precursor to membrane and storage lipids, and is thought to be present in the plastids and endoplasmic reticulum (ER) (Dolch & Maréchal, 2015). Although its exact localization in diatoms is not well known, PC is synthesized in the ER and thought to be the main extraplastidial lipid (Boudière et al., 2014; Dolch & Maréchal, 2015; Kroth et al., 2008). The storage lipid, TAG, exists in the form of droplets in *P. tricornutum* (Dolch & Maréchal, 2015). The increase of DBI in these non-thylakoid lipids and their importance to PET when PQ pool was oxidized is currently unclear. Nonetheless, the increase in DBIs appear to be specific as not all thylakoid lipids were affected indiscriminately. For instance, the DBI of PI, PE and DGTA were unchanged (Fig. 4a). Together, these data suggest a potential presence of a specific signaling mechanism in response to an oxidized PQ pool.

Many studies at a transcripional level of regulation of FADs have been reported using light and dark treatments (Bai et al., 2016; Collados et al., 2006; Hernández et al., 2011; Kis et al., 1998; Nishiuchi et al., 1995). However, light and dark can affect a host of cellular processes. Therefore, it is challenging to pinpoint the sensing signal(s) that regulates FADs. DNA microarray analyses of DCMU- and DBMIB-treated cyanobacteria suggest that FADs are redox-responsive (Hihara et al., 2003). However, the changes in expression were similarly repressed and this might be attributed to the physiological artifacts from the higher concentration of inhibitors used (an order of magnitude higher than the present study). A recent study in diatoms pointed out that lower light intensity led to decrease in fatty acid saturation, and vice versa (Conceição et al., 2020). However, the signal(s) that led to this observation remain elusive and unexplored. Diatoms are secondary endosymbionts that possess four layers of plastid envelope membranes (Bowler et al., 2008, 2010). Retrograde signaling was once considered to be unlikely in diatoms because a signal from plastids must travel through these membranes to the nucleus (Wilhelm et

al., 2006). However, a focused analysis of the diatom plastid shows that it is bound to the outer nuclear envelope (oNE) by a direct connection with its outermost membrane, namely the chloroplast endoplasmic reticulum membrane (cERM)(Flori et al., 2016) In addition, at the level of the oNE-cERM isthmus, a membrane contact site links tightly the second outermost membrane of the plastid i.e., the periplastidial membrane (PPM) with the inner nuclear envelope (iNE) (Flori et al., 2016) The oNE-cERM isthmus and the iNE-PPM membrane contact site are therefore physical connections, which might determine highly efficient plastid-nuclear interactions in diatoms. Here, our data suggest that the change in fatty acid profile is connected to the redox state of the PQ pool transcriptionally (Fig. 5). An oxidized PQ pool led to an initial increase in R of PAD by 3.3-fold at 6 h, which desaturates C16:0 to C16:1 (Smith et al., 2021). This increase in C16:1 may serve as the substrate for downstream fatty acid desaturation, which is reflected by the peak upregulation of most C16 FADs at 12 h. Once the new lipid homeostasis is achieved at 24 h, all FADs exhibited unchanged expression relative to the internal standard gene. Together with the corresponding GC-MS and LC-MS/MS data, this expression pattern, in which FADs was upregulated to attain a new state of lipid homeostasis and downregulated once homeostasis was attained, suggests that the redox state of the PQ pool may function as a retrograde signal to regulate nuclear-encoded FADs.

The connection between the redox state of the PQ pool and saturation state of thylakoid fatty acids may have important physiological implications to the organism. Many crucial processes in photosynthesis, such as PET and PSII repair, rely heavily on diffusion (Goral et al., 2010; Kirchhoff, 2014; Kirchhoff et al., 2000). In PET, PQ and its reduced form, PQH_2, are the only lipophilic mobile electron carriers that diffuse in the acyl tails of thylakoid lipids. Hence, decreased thylakoid fatty acid saturation induced by low light or DCMU (Fig. 1a, 2, 3a and 4a) is likely to decrease the viscosity of the microenvironment between PSII and cyt b_6f. This may promote the rate of diffusion of PQ and PQH_2 to encourage higher electron input to PET. Conversely, saturated thylakoid membranes may retard the rates of PQ and PQH_2 diffusion to restrict electron input to PET in cells exposed to high light or DBMIB. We also explored the possibility if the redox state of PQ pool can act as a thermal sensor to modulate the saturation level of thylakoid fatty acids. According to the photostasis theory, low temperature and high light, both similarly exert high excitation pressure at PSII (Ensminger et al., 2006; Huner et al., 1998, 2002; Wilson et al., 2006). Theoretically, DBMIB and low temperature treatments (inversely, DCMU and high temperature treatments) should result in similar fatty acid profiles. However, we did not observe these similarities in our cultures (data not shown). Thus, it is possible that additional sensors (or checks) are needed to trigger thermal modulation of thylakoid fatty acids. To the extent these experimental

353 results apply, the redox state of the PQ pool may serve as one of the signaling mechanisms to modulate
354 FADs.

355 An oxidized PQ pool increases the abundance of light-harvesting complexes and the associated
356 Chl *a* (Escoubas et al., 1995; Maxwell et al., 1995). In accordance with literature, we observed *ca.* 70%
357 increase in Chl *a* in DCMU-treated cells (Fig. S1). Instead of light harvesting complex II in terrestrial
358 plants, diatoms utilize fucoxanthin (Fx), chlorophyll a/c binding proteins (FCP) as the major peripheral
359 light harvesting antennae for the photosystems. There are eight molecules of Chl *a*, eight Fx and two Chl
360 *c* bound to each monomeric FCP (Premvardhan et al., 2010). Thus, a lack of corresponding increase in Fx
361 and Chl *c* suggests that oxidation of the PQ pool alone did not significantly increase the abundance of
362 FCPs, but mainly the reaction centers. According to the percolation diffusion theory, high protein density
363 encloses diffusion domain and prevents long-range diffusion of smaller hydrophobic molecules (Almeida
364 & Vaz, 1995; Kirchhoff, 2014; Saxton, 1989). Thus, an increase in the abundance of reaction centers,
365 with unchanged thylakoid lipid abundance, may increase thylakoid protein density and impede lateral
366 diffusion of lipophilic molecules. Thus, decreasing the saturation level of thylakoid fatty acids may
367 counter this increase in membrane viscosity, for maintenance of lateral diffusion in the hydrophobic
368 membrane core.

369 An oxidized PQ pool also led to changes in cellular lipid composition. We observed a *ca.* 60%
370 decrease in DGDG (Fig. 6a) and corresponding 1.74-fold increase in MGDG/DGDG (Fig. 6b). MGDG
371 (conical) does not promote bilayer forming whereas DGDG (cylindrical and forms hydrogen bonds with
372 polar heads of lipids in adjacent bilayers) does (Demé et al., 2014; Williams, 1998). MGDG tends to form
373 hexagonal II (HII) phase i.e., inverted tubules where lipid head groups form the center of the tubule and
374 fatty acids are pointing outward to the aqueous phase (Jouhet, 2013; Seddon, 1990; Shipley et al.,
375 1973). Decreasing saturation in fatty acids also favors the formation of the HII phase. Together, it
376 appears that thylakoid membranes may favor the HII phase but not the lamellar phase (bilayer-forming
377 and crucial for the maintenance of ultrastructure) when the PQ pool is oxidized. Data from ^{31}P-NMR
378 experiments on spinach thylakoids suggest that non-bilayer phases may play an important role in
379 structural dynamics of thylakoid membranes (Garab et al., 2017). HII phase is important for the activities
380 of some enzymes, including de-epoxidation of violaxanthin (Latowski et al., 2004). However, the cells
381 examined exhibited decreased abundance of Ddx and unchanged Dtx (Fig. S1). They did not appear to
382 activate non-photochemical quenching. Thus, this complex structure-function relationship of thylakoid
383 lipids remains enigmatic. In phosphorus limiting condition, deficiency in PC could be replaced by DGTA

(Abida et al., 2015). However, our cells were grown in nutrient replete condition and thus the link between the redox state of PQ pool to these lipids is unclear. Future study should focus on the roles of these lipids in photosynthesis, especially in PET. Although it may seem straightforward, changes in fatty acid saturation have profound structural implications to biophysical properties of thylakoid membranes. In an *Arabidopsis* mutant deficient in *fad5*, semicrystalline PSII arrays were observed (Tietz et al., 2015). Instead of impeding the diffusion of small lipophilic molecules, the authors reported an enhancement of mobility of PQ and xanthophylls due to altered supramolecular protein organization. In diatoms, cryo-ET studies revealed semicrystalline arrays of PSII core subunits (Levitan et al., 2019). It will be interesting to study the effects of the PQ redox state on the supramolecular organization of PSII and PET.

This work provides a reference for future studies on elucidating the molecular intermediates connecting the plastid signal to nuclear gene expression in this retrograde signaling pathway.

Acknowledgements

Funding was provided by the Bennett L. Smith endowment to PGF. We thank Nicole Waite and Grace Saba for assistance in HPLC analysis. We are grateful to Kevin Wyman for help in laboratory analyses. The LIPANG platform is supported by GRAL, financed within the University Grenoble Alpes graduate school (Ecole Universitaire de Recherche) CBH-EUR-GS (ANR-17-EURE-0003), and the Auvergne-Rhône-Alpes region with the European Union *via* the FEDER program.

Author contribution

All authors contributed to the study conception and design. Material preparation, data collection and analysis were performed by Kuan Yu Cheong and Juliette Jouhet. The first draft of the manuscript was written by Kuan Yu Cheong and all authors commented on previous versions of the manuscript. All authors read and approved the final manuscript.

Data availability

The data that support the findings of this study are available from the corresponding author upon reasonable request.

Code availability

Not applicable.

Declarations

Conflict of interest

The authors declare that they hae no confluct of interest.

References

Abdallah, F., Salamini, F., & Leister, D. (2000). A prediction of the size and evolutionary origin of the proteome of chloroplasts of Arabidopsis. *Trends in Plant Science*, *5*(4), 141–142.

Abida, H., Dolch, L., Meï, C., Villanova, V., Conte, M., Block, M. A., Finazzi, G., Bastien, O., Tirichine, L., Bowler, C., Rébeillé, F., Petroutsos, D., Jouhet, J., & Maréchal, E. (2015). Membrane Glycerolipid Remodeling Triggered by Nitrogen and Phosphorus Starvation in. *Plant Physiology*, *167*(1), 118–136. https://doi.org/10.1104/pp.114.252395

Allen, J. F., de Paula, W. B. M., Puthiyaveetil, S., & Nield, J. (2011). A structural phylogenetic map for chloroplast photosynthesis. *Trends in Plant Science*, *16*(12), 645–655.

Almeida, P. F. F., & Vaz, W. L. C. (1995). Lateral diffusion in membranes. In *Handbook of biological physics* (Vol. 1, pp. 305–357). Elsevier.

Bai, X., Song, H., Lavoie, M., Zhu, K., Su, Y., Ye, H., Chen, S., Fu, Z., & Qian, H. (2016). Proteomic analyses bring new insights into the effect of a dark stress on lipid biosynthesis in Phaeodactylum tricornutum. *Scientific Reports*, *6*(December 2015), 1–10. https://doi.org/10.1038/srep25494

Beck, J. G., Mathieu, D., Loudet, C., Buchoux, S., & Dufourc, E. J. (2007). Plant sterols in “rafts”: a better way to regulate membrane thermal shocks. *The FASEB Journal*, *21*(8), 1714–1723.

Bligh, E. G., & Dyer, W. J. (1959). A rapid method of total lipid extraction and purification. *Canadian Journal of Biochemistry and Physiology*, *37*(8), 911–917.

Block, M. A., Dorne, A., Joyard, J., & Douce, R. (1983). Preparation and characterization of membrane fractions enriched in outer and inner envelope membranes from spinach chloroplasts. II. Biochemical characterization. *Journal of Biological Chemistry*, *258*(21), 13281–13286.

Boudière, L., Michaud, M., Petroutsos, D., Rébeillé, F., Falconet, D., Bastien, O., Roy, S., Finazzi, G., Rolland, N., Jouhet, J., Block, M. A., & Maréchal, E. (2014). Glycerolipids in photosynthesis: composition, synthesis and trafficking. *Biochimica et Biophysica Acta (BBA)*, *1837*, 470–480.

Bowler, C., Allen, A. E., Badger, J. H., Grimwood, J., Jabbari, K., Kuo, A., Maheswari, U., Martens, C., Maumus, F., Otillar, R. P., Rayko, E., Salamov, A., Vandepoele, K., Beszteri, B., Gruber, A., Heijde, M., Katinka, M., Mock, T., Valentin, K., … Grigoriev, I. V. (2008). The Phaeodactylum genome reveals the evolutionary history of diatom genomes. *Nature*, *456*(7219), 239–244. https://doi.org/10.1038/nature07410

Bowler, C., Vardi, A., & Allen, A. E. (2010). Oceanographic and biogeochemical insights from diatom genomes. *Annual Review of Marine Science*, *2*, 333–365.

Budin, I., Rond, T. de, Chen, Y., Chan, L. J. G., Petzold, C. J., & Keasling, J. D. (2018). Viscous control of cellular respiration by membrane lipid composition. *Science*, *7925*(October), 1–10. https://doi.org/10.1126/science.aat7925

Buseman, C. M., Tamura, P., Sparks, A. A., Baughman, E. J., Maatta, S., Zhao, J., Roth, M. R., Esch, S. W., Shah, J., Williams, T. D., & others. (2006). Wounding stimulates the accumulation of glycerolipids

containing oxophytodienoic acid and dinor-oxophytodienoic acid in Arabidopsis leaves. *Plant Physiology*, *142*(1), 28–39.

Chen, Y. B., Durnford, D. G., Koblizek, M., & Falkowski, P. G. (2004). Plastid Regulation of Lhcb1 Transcription in the Chlorophyte Alga Dunaliella tertiolecta. *Plant Physiology*, *136*(3), 3737–3750. https://doi.org/10.1104/pp.104.038919

Collados, R., Andreu, V., Picorel, R., & Alfonso, M. (2006). A light-sensitive mechanism differently regulates transcription and transcript stability of ω3 fatty-acid desaturases (FAD3, FAD7 and FAD8) in soybean photosynthetic cell suspensions. In *FEBS Letters* (Vol. 580, Issue 20, pp. 4934–4940). https://doi.org/10.1016/j.febslet.2006.07.087

Conceição, D., Lopes, R. G., Derner, R. B., Cella, H., do Carmo, A. P. B., Montes D'Oca, M. G., Petersen, R., Passos, M. F., Vargas, J. V. C., Galli-Terasawa, L. V., & Kava, V. (2020). The effect of light intensity on the production and accumulation of pigments and fatty acids in Phaeodactylum tricornutum. *Journal of Applied Phycology*, *3*. https://doi.org/10.1007/s10811-019-02001-6

Demé, B., Cataye, C., Block, M. A., Maréchal, E., & Jouhet, J. (2014). Contribution of galactoglycerolipids to the 3-dimensional architecture of thylakoids. *FASEB Journal*, *28*(8), 3373–3383. https://doi.org/10.1096/fj.13-247395

Diner, B., & Joliot, P. (1976). Effect of the transmembrane electric field on the photochemical and quenching properties of Photosystem II in vivo. *Biochimica et Biophysica Acta (BBA) - Bioenergetics*, *423*(3), 479–498. https://doi.org/https://doi.org/10.1016/0005-2728(76)90202-4

Dolch, L. J., & Maréchal, E. (2015). Inventory of fatty acid desaturases in the pennate diatom Phaeodactylum tricornutum. *Marine Drugs*, *13*(3), 1317–1339. https://doi.org/10.3390/md13031317

Douce, R., Alban, C., Bligny, R., Block, M. A., Covès, J., Dorne, A.-J., Journet, E.-P., Joyard, J., Neuburger, M., & Rebeillé, F. (1987). Lipid distribution and synthesis within the plant cell. In *The metabolism, structure, and function of plant lipids* (pp. 255–263). Springer.

Dufourc, E. J. (2008a). Sterols and membrane dynamics. *Journal of Chemical Biology*, *1*(1–4), 63–77.

Dufourc, E. J. (2008b). The role of phytosterols in plant adaptation to temperature. *Plant Signaling & Behavior*, *3*(2), 133–134.

Durnford, D. G., Prasil, O., Escoubas, J.-M., & Falkowski, P. G. (1998). [15] Assessing the potential for chloroplast redox regulation of nuclear gene expression. *Methods in Enzymology*, *297*, 220–234.

Ensminger, I., Busch, F., & Huner, N. P. A. (2006). Photostasis and cold acclimation: Sensing low temperature through photosynthesis. *Physiologia Plantarum*, *126*(1), 28–44. https://doi.org/10.1111/j.1399-3054.2006.00627.x

Escoubas, J. M., Lomas, M., LaRoche, J., & Falkowski, P. G. (1995). Light intensity regulation of cab gene transcription is signaled by the redox state of the plastoquinone pool. *Proceedings of the National Academy of Sciences*, *92*(22), 10237–10241. https://doi.org/10.1073/pnas.92.22.10237

Fedtke, C. (1982). Approaches to and Definitions of the Mechanisms of Action of Herbicides. In C. Fedtke (Ed.), *Biochemistry and Physiology of Herbicide Action* (pp. 1–14). Springer.

Feijão, E., Gameiro, C., Franzitta, M., Duarte, B., Caçador, I., Cabrita, M. T., & Matos, A. R. (2017). Heat wave impacts on the model diatom Phaeodactylum tricornutum: Searching for photochemical and fatty acid biomarkers of thermal stress. *Ecological Indicators*, *March*, 0–1. https://doi.org/10.1016/j.ecolind.2017.07.058

Flori, S., Jouneau, P.-H., Finazzi, G., Maréchal, E., & Falconet, D. (2016). Ultrastructure of the Periplastidial Compartment of the Diatom Phaeodactylum tricornutum. *Protist*, *167*(3), 254–267. https://doi.org/10.1016/j.protis.2016.04.001

Garab, G., Ughy, B., De Waard, P., Akhtar, P., Javornik, U., Kotakis, C., Šket, P., Karlick\`y, V., Materová, Z., Špunda, V., & others. (2017). Lipid polymorphism in chloroplast thylakoid membranes--as revealed by 31 P-NMR and time-resolved merocyanine fluorescence spectroscopy. *Scientific Reports*, *7*(1), 1–11.

Goral, T. K., Johnson, M. P., Brain, A. P. R., Kirchhoff, H., Ruban, A. V., & Mullineaux, C. W. (2010). Visualizing the mobility and distribution of chlorophyll proteins in higher plant thylakoid membranes: Effects of photoinhibition and protein phosphorylation. *Plant Journal*, *62*(6), 948–959. https://doi.org/10.1111/j.1365-313X.2010.04207.x

Gorbunov, M. Y., & Falkowski, P. G. (2020). Using chlorophyll fluorescence kinetics to determine photosynthesis in aquatic ecosystems. *Limnology and Oceanography*. https://doi.org/doi:10.1002/lno.11581

Grzebyk, D., Schofield, O., Vetriani, C., & Falkowski, P. G. (2003). The mesozoic radiation of eukaryotic algae: the portable plastid hypothesis. *Journal of Phycology*, *39*(2), 259–267.

Guillard, R. R. (1975). Culture of phytoplankton for feeding marine invertebrates. In *Culture of phytoplankton for feeding marine invertebrates.* (pp. 29–60). Springer.

Guillard, R. R. L. (1973). Division rates. In *Handbook of phycological methods: culture methods and growth measurements* (pp. 289– 312). Cambridge University Press.

Guillard, R. R., & Ryther, J. H. (1962). Studies of marine planktonic diatoms: I. Cyclotella nana Hustedt, and Detonula confervacea (Cleve) Gran. *Canadian Journal of Microbiology*, *8*(2), 229–239.

Haehnel, W. (1977). Electron transport between plastoquinone and chlorophyll A1 in chloroplasts. II. Reaction kinetics and the function of plastocyanin in situ. *Biochimica et Biophysica Acta (BBA)-Bioenergetics*, *459*(3), 418–441.

Harwood, J. L., & Jones, A. L. (1989). *Lipid Metabolism in Algae* (J. A. Callow, Ed.; Vol. 16, pp. 1–53). Academic Press. https://doi.org/https://doi.org/10.1016/S0065-2296(08)60238-4

Hernández, M. L., Padilla, M. N., Sicardo, M. D., Mancha, M., & Martínez-Rivas, J. M. (2011). Effect of different environmental stresses on the expression of oleate desaturase genes and fatty acid composition in olive fruit. *Phytochemistry*, *72*(2–3), 178–187. https://doi.org/10.1016/j.phytochem.2010.11.026

Hihara, Y., Sonoike, K., Kanehisa, M., & Ikeuchi, M. (2003). DNA Microarray Analysis of Redox-Responsive Genes in the Genome of the Cyanobacterium Synechocystis sp. Strain PCC 6803. *The Journal of Bacteriology*, *185*(5), 1719–1725. https://doi.org/10.1128/JB.185.5.1719

Horváth, G., Droppa, M., Szitó, T., Mustárdy, L., Horváth, L., & Vigh, L. (1986). Homogeneous catalytic hydrogenation of lipids in the photosynthetic membrane: effects on membrane structure and photosynthetic activity. *Biochimica et Biophysica Acta (BBA)-Bioenergetics*, *849*(3), 325–336.

Huner, N. P. A., Ivanov, A. G., Wilson, K. E., Miskiewicz, E., & Krol, M. (2002). Energy sensing and photostasis in photoautotrophs. In *Cell and molecular responses to stress* (pp. 243–255).

Huner, N. P. A., Öquist, G., & Sarhan, F. (1998). Energy balance and acclimation to light and cold. *Trends in Plant Science*, *3*(6), 224–230.

Jenke, D., & Odufu, A. (2012). Utilization of internal standard response factors to estimate the concentration of organic compounds leached from pharmaceutical packaging systems and application of such estimated concentrations to safety assessment. *Journal of Chromatographic Science*, *50*(3), 206–212. https://doi.org/10.1093/chromsci/bmr048

Jouhet, J. (2013). Importance of the hexagonal lipid phase in biological membrane organization. *Frontiers in Plant Science*, *4*(DEC), 1–5. https://doi.org/10.3389/fpls.2013.00494

Jouhet, J., Lupette, J., Clerc, O., Magneschi, L., Bedhomme, M., Collin, S., Roy, S., Maréchal, E., & Rebeille, F. (2017). LC-MS/MS versus TLC plus GC methods: consistency of glycerolipid and fatty acid profiles in microalgae and higher plant cells and effect of a nitrogen starvation. *PLoS One*, *12*(8), e0182423.

Karpinski, S., Escobar, C., Karpinska, B., Creissen, G., & Mullineaux, P. M. (1997). Photosynthetic electron transport regulates the expression of cytosolic ascorbate peroxidase genes in arabidopsis during excess light stress. *Plant Cell*, *9*(4), 627–640. https://doi.org/10.1105/tpc.9.4.627

Khorobrykh, S., Tsurumaki, T., Tanaka, K., Tyystjärvi, T., & Tyystjärvi, E. (2020). Measurement of the redox state of the plastoquinone pool in cyanobacteria. *FEBS Letters*, *594*(2), 367–375.

Kirchhoff, H. (2014). Diffusion of molecules and macromolecules in thylakoid membranes. *Biochimica et Biophysica Acta - Bioenergetics*, *1837*(4), 495–502. https://doi.org/10.1016/j.bbabio.2013.11.003

Kirchhoff, H., Horstmann, S., & Weis, E. (2000). Control of the photosynthetic electron transport by PQ diffusion microdomains in thylakoids of higher plants. *Biochimica et Biophysica Acta - Bioenergetics*, *1459*(1), 148–168. https://doi.org/10.1016/S0005-2728(00)00143-2

Kis, M., Zsiros, O., Farkas, T., Wada, H., Nagy, F., & Gombos, Z. (1998). Light-induced expression of fatty acid desaturase genes. *Proceedings of the National Academy of Sciences*, *95*(8), 4209–4214. https://doi.org/10.1073/pnas.95.8.4209

Kolber, Z. S., Prášil, O., & Falkowski, P. G. (1998). Measurements of variable chlorophyll fluorescence using fast repetition rate techniques: defining methodology and experimental protocols. *Biochimica et Biophysica Acta (BBA)-Bioenergetics*, *1367*(1–3), 88–106.

559 Kroth, P. G., Chiovitti, A., Gruber, A., Martin-Jezequel, V., Mock, T., Parker, M. S., Stanley, M. S., Kaplan,
560 A., Caron, L., Weber, T., & others. (2008). A model for carbohydrate metabolism in the diatom
561 Phaeodactylum tricornutum deduced from comparative whole genome analysis. *PloS One*, *3*(1),
562 e1426.

563 Latowski, D., Åkerlund, H.-E., & Strzałka, K. (2004). Violaxanthin de-epoxidase, the xanthophyll cycle
564 enzyme, requires lipid inverted hexagonal structures for its activity. *Biochemistry*, *43*(15), 4417–
565 4420.

566 Lepetit, B., Sturm, S., Rogato, A., Gruber, A., Sachse, M., Falciatore, A., Kroth, P. G., & Lavaud, J. (2012).
567 High Light Acclimation in the Secondary Plastids Containing Diatom Phaeodactylum tricornutum is
568 Triggered by the Redox State of the Plastoquinone Pool. *Plant Physiology*, *161*(2), 853–865.
569 https://doi.org/10.1104/pp.112.207811

570 Levitan, O., Chen, M., Kuang, X., Cheong, K. Y., Jiang, J., Banal, M., Nambiar, N., Gorbunov, M. Y., Ludtke,
571 S. J., Falkowski, P. G., & Dai, W. (2019). Structural and functional analyses of photosystem II in the
572 marine diatom Phaeodactylum tricornutum. *Proceedings of the National Academy of Sciences of*
573 *the United States of America*, *116*(35), 17316–17322. https://doi.org/10.1073/pnas.1906726116

574 Li, H., & Sherman, L. A. (2000). A redox-responsive regulator of photosynthesis gene expression in the
575 cyanobacterium Synechocystis sp. Strain PCC 6803. *Journal of Bacteriology*, *182*(15), 4268–4277.
576 https://doi.org/10.1128/JB.182.15.4268-4277.2000

577 Martin, W., Rujan, T., Richly, E., Hansen, A., Cornelsen, S., Lins, T., Leister, D., Stoebe, B., Hasegawa, M.,
578 & Penny, D. (2002). Evolutionary analysis of Arabidopsis, cyanobacterial, and chloroplast genomes
579 reveals plastid phylogeny and thousands of cyanobacterial genes in the nucleus. *Proceedings of the*
580 *National Academy of Sciences*, *99*(19), 12246–12251.

581 Maxwell, D. P., Falk, S., Trick, C. G., & Huner, N. P. A. (1994). Growth at Low Temperature Mimics High-
582 Light Acclimation in Chlorella vulgaris. *Plant Physiology*, *105*(2), 535–543.
583 https://doi.org/10.1104/pp.105.2.535

584 Maxwell, D. P., Laudenbach, D. E., & Huner, N. P. A. (1995). Redox Regulation of Light-Harvesting
585 Complex II and cab mRNA Abundance in Dunaliella salina. *Plant Physiology*, *109*(3), 787–795.
586 https://doi.org/10.1104/pp.109.3.787

587 Mendiola-Morgenthaler, L., Eichenberger, W., & Boschetti, A. (1985). Isolation of chloroplast envelopes
588 from Chlamydomonas. Lipid and polypeptide composition. *Plant Science*, *41*(2), 97–104.

589 Nakamura, Y., & Li-Beisson, Y. (2016). *Lipids in plant and algae development* (Vol. 86). Springer.

590 Nishiuchi, T., Nakamura, T., Abe, T., Kodama, H., Nishimura, M., & Iba, K. (1995). Tissue-specific and
591 light-responsive regulation of the promoter region of the Arabidopsis thaliana chloroplast ω-3 fatty
592 acid desaturase gene (FAD7). *Plant Molecular Biology*, *29*(3), 599–609.
593 https://doi.org/10.1007/BF00020987

594 Öquist, G. (1982). Seasonally Induced Changes in Acyl Lipids and Fatty-Acids of Chloroplast Thylakoids of
595 Pinus-Silvestris - a Correlation Between the Level of Unsaturation of Monogalactosyldiglyceride
596 and the Rate of Electron-Transport. *Plant Physiology*, *69*(4), 869–875.

Oudot-Le Secq, M.-P., Grimwood, J., Shapiro, H., Armbrust, E. V., Bowler, C., & Green, B. R. (2007). Chloroplast genomes of the diatoms Phaeodactylum tricornutum and Thalassiosira pseudonana: comparison with other plastid genomes of the red lineage. *Molecular Genetics and Genomics*, *277*(4), 427–439.

Pfaffl, M. W. (2001). A new mathematical model for relative quantification in real-time RT – PCR. *Nucleic Acids Research*, *29*(9), 16–21.

Pfannschmidt, T., Nilsson, A., & Allen, J. F. (1999). Photosynthetic control of chloroplast gene expression. *Nature*, *397*(6720), 625–628. https://doi.org/10.1038/17624

Premvardhan, L., Robert, B., Beer, A., & Büchel, C. (2010). Pigment organization in fucoxanthin chlorophyll a/c2 proteins (FCP) based on resonance Raman spectroscopy and sequence analysis. *Biochimica et Biophysica Acta (BBA)-Bioenergetics*, *1797*(9), 1647–1656.

Rainteau, D., Humbert, L., Delage, E., Vergnolle, C., Cantrel, C., Maubert, M.-A., Lanfranchi, S., Maldiney, R., Collin, S., Wolf, C., & others. (2012). Acyl chains of phospholipase D transphosphatidylation products in Arabidopsis cells: a study using multiple reaction monitoring mass spectrometry. *PLoS One*, *7*(7), e41985.

Rodríguez-Ruiz, J., Belarbi, E. H., Sánchez, J. L. G., & Alonso, D. L. (1998). Rapid simultaneous lipid extraction and transesterification for fatty acid analyses. *Biotechnology Techniques*, *12*(9), 689–691. https://doi.org/10.1023/A:1008812904017

Rujan, T., & Martin, W. (2001). How many genes in Arabidopsis come from cyanobacteria? An estimate from 386 protein phylogenies. *TRENDS in Genetics*, *17*(3), 113–120.

Sarcina, M., Murata, N., Tobin, M. J., & Mullineaux, C. W. (2003). Lipid diffusion in the thylakoid membranes of the cyanobacterium Synechococcus sp.: Effect of fatty acid desaturation. *FEBS Letters*, *553*(3), 295–298. https://doi.org/10.1016/S0014-5793(03)01031-7

Saxton, M. J. (1989). Lateral diffusion in an archipelago. Distance dependence of the diffusion coefficient. *Biophysical Journal*, *56*(3), 615–622.

Seddon, J. M. (1990). Structure of the inverted hexagonal (HII) phase, and non-lamellar phase transitions of lipids. *Biochimica et Biophysica Acta (BBA)-Reviews on Biomembranes*, *1031*(1), 1–69.

Shipley, G. G., Green, J. P., & Nichols, B. W. (1973). The phase behavior of monogalactosyl, digalactosyl, and sulphoquinovosyl diglycerides. *Biochimica et Biophysica Acta (BBA)-Biomembranes*, *311*(4), 531–544.

Siaut, M., Heijde, M., Mangogna, M., Montsant, A., Coesel, S., Allen, A., Manfredonia, A., Falciatore, A., & Bowler, C. (2007). Molecular toolbox for studying diatom biology in Phaeodactylum tricornutum. *Gene*, *406*(1–2), 23–35.

Smith, R., Jouhet, J., Gandini, C., Nekrasov, V., Marechal, E., Napier, J. A., & Sayanova, O. (2021). Plastidial acyl carrier protein Δ9-desaturase modulates eicosapentaenoic acid biosynthesis and triacylglycerol accumulation in Phaeodactylum tricornutum. *The Plant Journal*, *106*(5), 1247–1259. https://doi.org/10.1111/tpj.15231

634 Sunda, W. G., Price, N. M., & Morel, F. M. M. (2005). Trace metal ion buffers and their use in culture
635 studies. *Algal Culturing Techniques*, *4*, 35–63.

636 Tietz, S., Puthiyaveetil, S., Enlow, H. M., Yarbrough, R., Wood, M., Semchonok, D. A., Lowry, T., Li, Z.,
637 Jahns, P., Boekema, E. J., Lenhert, S., Niyogi, K. K., & Kirchhoff, H. (2015). Functional implications of
638 photosystem II crystal formation in photosynthetic membranes. *Journal of Biological Chemistry*,
639 *290*(22), 14091–14106. https://doi.org/10.1074/jbc.M114.619841

640 Trebst, A. (2007). Inhibitors in the functional dissection of the photosynthetic electron transport system.
641 *Photosynthesis Research*, *92*(2), 217–224. https://doi.org/10.1007/s11120-007-9213-x

642 Valentin, K., Cattolico, R. A., & Zetsche, K. (1992). Phylogenetic origin of the plastids. In *Origins of*
643 *plastids* (pp. 193–221). Springer.

644 Vigh, L., Joo, F., Droppa, M., Horvath, L. I., & Horvath, G. (1985). Modulation of chloroplast membrane
645 lipids by homogeneous catalytic hydrogenation. *European Journal of Biochemistry*, *147*(3), 477–
646 481.

647 Wilhelm, C., Büchel, C., Fisahn, J., Goss, R., Jakob, T., LaRoche, J., Lavaud, J., Lohr, M., Riebesell, U.,
648 Stehfest, K., & others. (2006). The regulation of carbon and nutrient assimilation in diatoms is
649 significantly different from green algae. *Protist*, *157*, 91–124.

650 Williams, W. P. (1998). The physical properties of thylakoid membrane lipids and their relation to
651 photosynthesis. In *In Lipids in photosynthesis: structure, function and genetics* (pp. 103–118).
652 Springer.

653 Wilson, K. E., Ivanov, A. G., Öquist, G., Grodzinski, B., Sarhan, F., & Huner, N. P. A. (2006). Energy
654 balance, organellar redox status, and acclimation to environmental stress. *Botany*, *84*(9), 1355–
655 1370.

656 Wright, S. W., Jeffrey, S. W., Mantoura, R. F. C., Llewellyn, C. A., Bjørnland, T., Repeta, D., &
657 Welschmeyer, N. (1991). Improved HPLC method for the analysis of chlorophylls and carotenoids
658 from marine phytoplankton. *Marine Ecology Progress Series*, 183–196.

659 Yang, D.-H., Andersson, B., Aro, E.-M., & Ohad, I. (2001). The redox state of the plastoquinone pool
660 controls the level of the light-harvesting chlorophyll a/b binding protein complex II (LHC II) during
661 photoacclimation. *Photosynthesis Research*, *68*(2), 163–174.

662

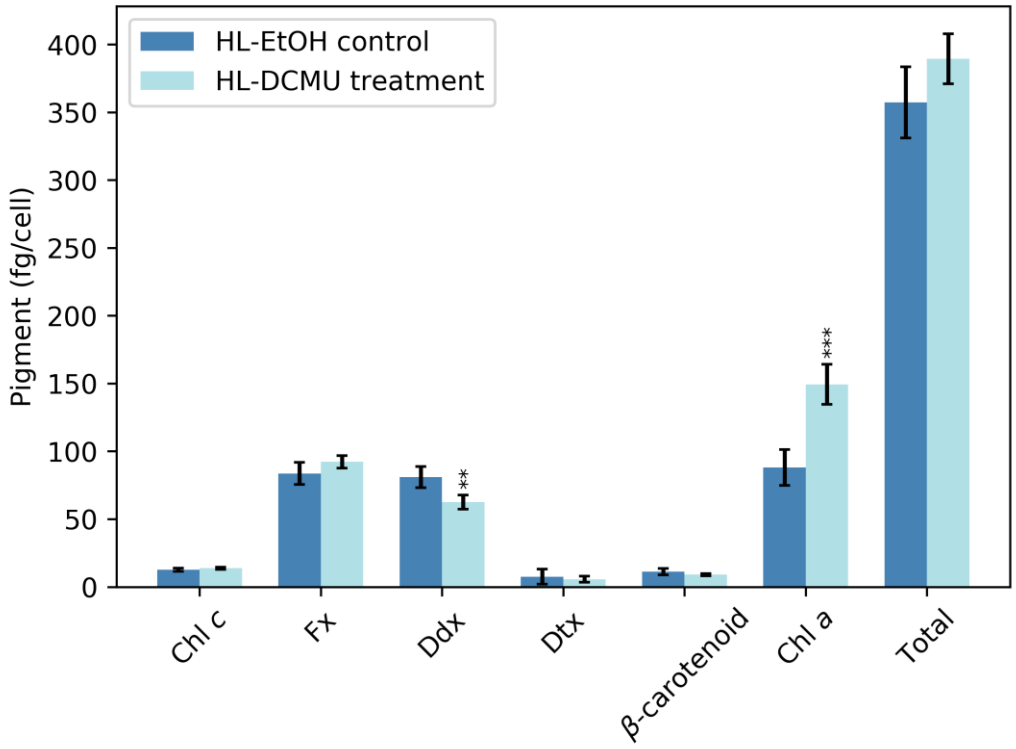

663

664 **Supporting Information Fig. S1. Pigment composition of *P. tricornutum* incubated with 25 nM of 3-**
665 **(3,4-dichlorophenyl)-1,1-dimethylurea (DCMU) for 24 h.** Data collected by high-performance liquid
666 chromatography (HPLC). Values reported are means ± standard deviation (n = 4 biological replicates).
667 "*" represents $p \leqslant 0.05$, "**" represents $p \leqslant 0.01$ and "***" represents $p \leqslant 0.001$ ($\alpha = 0.05$ with
668 independent t-test). Abbreviation: Chl *c*, chlorophyll *c*; Fx, fucoxanthin; Ddx, diadinoxanthin; Dtx,
669 Diatoxanthin; Chl *a*, chlorophyll *a*.

670 **Supporting Information Table S1. Primer sequences used for RT-qPCR.**

Gene	**Ensembl Protists ID**	**Strand**	**Sequence (5'-3')**
RPS (ribosomal protein small subunit 30S)	Phatr3_J10847	Forward	CGAAGTCAACCAGGAAACCAA
RPS (ribosomal protein small subunit 30S)	Phatr3_J10847	Reverse	GTGCAAGAGACCGGACATACC
PAD	Phatr3_J9316	Forward	TGCGGTGCTTGCCTTTC
PAD	Phatr3_J9316	Reverse	ACCCCGCAGATGTCTTCGTA

PTD12	Phatr3_J48423	Forward	CGATAAGGAGGGCGAGAAGA
PTD12	Phatr3_J48423	Reverse	CCGGTCGCACCGATCA
Putative C16:2 to C16:3 desaturase	Phatr3_EG02619	Forward	CTTCCCGCGATCTTTTTGAG
Putative C16:2 to C16:3 desaturase	Phatr3_EG02619	Reverse	TGACCCAATCTGGCTGATAAGTT
PTD15	Phatr3_J41570	Forward	AGTGACGTTGAATGCCAAAAGA
PTD15	Phatr3_J41570	Reverse	ATCCCGTCGAGGATGGATTT

671